

# 1 **A modular library for fast prototyping of solution-state nuclear** 2 **magnetic resonance experiments**

3 Michał Górka, Wiktor Koźmiński

4 Biological and Chemical Research Centre, Faculty of Chemistry, University of Warsaw, Żwirki i Wigury 101, 02-089  
5 Warsaw, Poland

6

7 *Correspondence to:* Wiktor Koźmiński (kozmin@chem.uw.edu.pl)

8 **Abstract.** We present a framework library (Modular Elements, ME) for the development of pulse sequences for Bruker  
9 spectrometers. It implements a two-level abstraction approach—the lower level comprises basic functional elements of pulse  
10 sequences and the higher one often-reused blocks comprising several evolution periods. The low-level abstractions reduce  
11 code duplication between variants of experiments such as hard-pulse and selective variants of individual NMR experiments.  
12 The high-level modules enable further reuse of pulse program code and aid in the construction of complex experiments. We  
13 show the library’s functionality by presenting pulse programs that can be switched between standard and TROSY variants,  
14 hard and shaped pulses and can seamlessly incorporate real-time homodecoupling. Adaptability is further demonstrated in a  
15 configurable 4D NOESY program.

## 16 **1 Introduction**

17 NMR is an extraordinarily powerful and adaptable spectroscopic method, with just the solution-state variant being capable of  
18 discerning the structure and dynamics of molecules ranging in size from simple organic compounds to large protein  
19 complexes such as a proteasome (Sprangers and Kay, 2007). The variety of experimental objects and the great number of  
20 parameters that can be measured has led to the proliferation of not only general experimental schemes, such as an  $^1\text{H}$ ,  $^{15}\text{N}$   
21 HSQC (Bodenhausen and Ruben, 1980) or a HNC0 (Kay et al., 1990b; Ikura et al., 1990), but also their variants and thus  
22 the pulse sequences, implementing them as computer code. As an example, for the often used HNC0 experiment, the non-  
23 exhaustive list of meaningful implementation choices is: the experiment can use hard pulses or avoid saturating water using  
24 selective pulses (Schanda et al., 2006); the final transfer element can be a simple spin-echo (Palmer et al., 1991), a set of  
25 three echoes implementing a sensitivity-enhanced transfer or one of many TROSY variants (Salzmann et al., 1999b;  
26 Nietlispach, 2005), with possible optimizations (Salzmann et al., 1999a; Schulte-Herbrüggen and Sørensen, 2000); radiation  
27 damping can be suppressed with bipolar gradients (Sklenar, 1995). Even without implementing all specialised experiment  
28 variants, the standard library supplied with the TopSpin software (Bruker) contains over a thousand pulse programs.

29 A common problem with pulse sequences, especially in biological NMR, is thus the requirement to code multiple variants of  
30 a given sequence. If this is done in separate files (as in the TopSpin built-in library) it results in a lot of code repetition and if  
31 made using conditional statements, it can substantially complicate the structure of the file, making trouble-shooting harder.  
32 Similarly, many pulse sequences share large amounts of code, often with no or minimal changes. Because this repeated code  
33 is scattered across different sequences and variants of experiments adding new variants (using different soft pulses, adding  
34 homodecoupling) requires applying the same modification across a large part of the whole pulse sequence library, which is  
35 tedious and error-prone. It is possible to implement such a library using standard systems programming language like C or  
36 Python, but we decided to use the native programming language of the spectrometer system, since any user writing pulse  
37 sequence needs to be familiar with it and requiring knowledge of separate programming language and its tooling would be  
38 an unnecessary hurdle to adoption. Here we show that by abstracting certain functionality using the somewhat limited macro  
39 and "define" functionality built into the TopSpin software, the above-described problems can still be avoided and the code  
40 can be made more readable and easier to modify. Here, we present the Modular Elements (ME) library for Bruker  
41 spectrometers. Although the library is specific to a particular hardware vendor, the modular approach it implements is more  
42 general and can be implemented on other instruments. A previous implementation of a modular library for pulse program  
43 implementation (NMR blocks) can be found in (Zawadzka-Kazimierczuk, 2012) for Varian/Agilent spectrometers, where  
44 evolution periods such as INEPT or COS-INEPT were abstracted as C functions. Alternative approaches to a modular  
45 library include domain specific pulse program generators, like GENESIS (Yong et al., 2022) for NOAH supersequences.  
46 Specialized libraries combining custom pulse programs and various tools (Favier and Brutscher, 2019; Vallet et al., 2020;  
47 Lukavsky and Puglisi, 2001), are suitable for routine use, but have limited applicability in the prototyping of new sequences.

## 48 **2 General approach to pulse sequence modularisation**

49 We categorise the library's functionality as low- and high-level. Low-level functionality encompasses the creation of  
50 variables and functions (technically functional macros), abstracting the basic building blocks of pulse sequences like pulses,  
51 gradients and delays. A pulse function can expand to a 90 degree proton hard pulse or an HN selective excitation pulse  
52 depending on global settings. A gradient function can expand to "no operation" in standard HSQC, or a selection gradient in  
53 the gradient-selected HSQC variant, with its corresponding delay variable containing a zero or correspondingly non-zero  
54 length of time. Decoupling functions for protons and deuterium can likewise be enabled and disabled depending on whether  
55 a TROSY variant is desired and if the sample is deuterated. This functionality simplifies the writing of pulse sequences  
56 implementing multiple variants of a given NMR experiment and gives its user the ability to easily test and compare the  
57 effectiveness of the variants for a given sample and the commonization of parameters across variants enables faster  
58 optimisation.

59 High-level functionality is implemented as modules that are included in the pulse sequences and can be classified as general  
60 modules and specific modules. General modules implement elements common to almost all pulse sequences. The

61 functionally most significant ones are the preparation and acquisition modules. The preparation module gives the user the  
62 option to turn on functionality such as solvent presaturation or a combination of N/C pulses and pulse field gradients for  
63 spoiling of residual magnetisation on those nuclei. The acquisition module enables switching between standard or  
64 homodecoupled data acquisition. The specific modules are abstract blocks of pulse sequence elements that appear in many  
65 pulse sequences in an almost identical form. Two main types of specific modules are proximal and distal modules,  
66 abstracting the functionality of blocks including and following first excitation (distal) and right before acquisition  
67 (proximal). Despite a large variety of possible implementations, the proximal/distal fragments differentiate variants of a  
68 pulse sequence (for example a standard hard-pulse HNCO, selective/BEST-HNCO, hard pulse and BEST TROSY-HNCO  
69 (Solyom et al., 2013)) and the actual code is usually repeatable across different sequences. HNCO, HNCACO and HNCOCA  
70 (Yang and Kay, 1999) have very similar proximal and distal parts; HN(CA)CONH and HabCabCONH (Kazimierczuk et al.,  
71 2010) have different proximal blocks, but the distal block is still very similar for all sequences listed. With the use of the  
72 low-level functionality described above a single proximal module can abstract the initial two transfer periods (first with  
73 transverse H magnetisation and second with transverse N/C magnetisation), with the choice of N/C nucleus and choice of  
74 evolved J coupling (CO in HNCO) made using define directives in the main pulse sequence. NOESY experiments are  
75 particularly susceptible to modularisation, with the NOE transfer period naturally splitting them into proximal and distal  
76 blocks. Standard 2D experiments of the HSQC, TROSY and HMQC type have thus been implemented as proximal modules,  
77 that can be used on their own as 2D experiments or included in a 3 or 4D NOESY (Kay et al., 1990a) with the chosen distal  
78 modules, which can themselves be modified 2D experiments or simpler blocks.

### 79 **3 Library implementation**

80 Description of implementation details and design choices requires a quick recapitulation of TopSpin pulse programs'  
81 language specifics. TopSpin has two types of variables: user-adjustable numbered variables (*d1..d63* for delays,  
82 *cnst1...cnst63* for floating point constants, similarly for integer constants ("loopcounters") *lN*, pulse lengths *pN*, ...) and  
83 named variables (pulses, delays and loopcounters only, also lists of various kinds), which can only be manipulated within a  
84 pulse program. Some less-documented observations on the limitations of named variables are compiled in SI. TopSpin  
85 implements limited functionality for defining text-substitution macros ("--traditional" mode of the GNU C preprocessor *cpp*  
86 (Stallman and GCC Developer Community, 2012)), which can be used everywhere outside a "relation" (variable value  
87 calculations using a subset of C syntax), due to their implementation as text in quotes (treated as string literals by *cpp* and  
88 ignored for macro expansion), though this limitation can be overcome (see the file "notes on TopSpin.txt" in the ME library).  
89 The user can provide custom option choices to a pulse program using the ZGOPNTS variable to define appropriate macros.

## 90 3.1 Low-level modularisation

### 91 3.1.1 Variables

92 With no user-adjustable named variables, two approaches to making them consistent across different pulse programs are  
93 possible - indirection through named variables or introducing a convention attaching constant meaning to numbered  
94 variables. Due to the limited number and type of named variables, we predominantly use the latter option (with sets of  
95 variables described in files such as `delays.incl`, `pulse.incl`, ...) with some focused use of indirection - for example, proximal  
96 type modules use `timeHX` and `timeXY` for J coupling evolution times between the H, X and Y nuclei. Default values for all  
97 such variables can be set using the `me.set_parameters.py` TopSpin program. For variables that don't ordinarily have  
98 calculations performed on them (pulse phases `phN`, gradient programs `gpN`) we implemented full indirection, where the user  
99 can use `phFree1` or `phFree3` without worrying as to which `phN` variables are used by other parts of a pulse program.

### 100 3.1.2 Pulses

101 The most important low-level abstractions are pulse functions. They are implemented using function-like macros of `cpp` and  
102 have the general form of `nucleus_type(phase)`, where `nucleus` can be a general specifier like `H/C/N` or more specific like  
103 `HN/HC/CA/CO` and `type` is classified based on the desired functionality, with the main ones being: excitation (for the  
104 excitation of longitudinal magnetization), flipback (acting on transverse magnetization), refocussing, inversion (inverting  
105 longitudinal magnetization), `excitation_UR` and `flipback_UR` (implementing universal rotations). The pulse macros will have  
106 different replacement text based on global settings (usually `ZGOPTNS`). A proton pulse `"H_excitation(ph)"` will be replaced  
107 by a hard pulse `"p1 ph p1"` by default, but with a `"-DH_SHAPED"` option will instead be replaced by `"p54:sp54 ph"` for a  
108 selective soft pulse and the associated named variable `ph_excitation` will be set to have the same value as `p1` or `p54`.

109 Pulse programs should account for the effective evolution time during pulse (which can be as much as 1 ms for longer  
110 selective pulses) to give correctly phased spectra and optimal J coupling evolution times. This library only accounts for  
111 linear phase slope using the modelling method described in (Lescop et al., 2010), that is treating a pulse as sequence (delay,  
112 ideal pulse, delay), which accounts for the phase slope of many commonly used pulses and can be explicitly optimized for  
113 during pulse design (Gershenson et al., 2008; Asami et al., 2018). This phase slope is compensated for using variables such  
114 as `eH_excitation`, which for the hard pulse above would be set to  $\frac{2p1}{\pi}$ . We assume that the flipback and flipback\_UR pulses  
115 act as if they were time-reversed excitation pulses and so the effective evolution time for a flipback pulse acting on  
116 transverse magnetization is also `eH_excitation`. A `H_excitation_UR` pulse of phase `x` will give an effective time of  
117 `eH_excitation` for z magnetization, `eH_flipback` for y magnetization and `eH_excitation + eH_flipback` for x magnetization.  
118 By compensating delays using the above mentioned variables, the whole sequence can be switched from a hard pulse  
119 implementation to a shaped pulse version, whether to account for field inhomogeneity or perform band-selective excitation.

### 120 3.1.3 Code blocks

121 There are many small blocks of code that can be included/excluded in a pulse program based on a sequence variant. To limit  
122 the number of conditional statements in the main pulse program, many are defined as macros that will expand to pulse  
123 program code based on options, for example “H2O\_FLIPBACK(ph2)” will be replaced by “(11:sp1 ph2):f1” in a pulse  
124 sequence with water flipback and by whitespace if using selective pulses. Similarly DECOUPLE\_H\_ON and  
125 DECOUPLE\_H\_OFF macros will turn on proton decoupling in a standard HNC0 experiment but will have no effect in  
126 TROSY-HNC0.

### 127 3.2 High-level modularization

128 TopSpin pulse programs follow a defined sequential structure that complicates the implementation of high-level modules as  
129 individual files and, in general, is:

- 130 1) configuration and compile-time calculations
- 131 2) a "zd" or "ze" statement
- 132 3) pulse program body (pulses and delays) and real-time calculations
- 133 4) signal acquisition block
- 134 5) loop statements for scans of a FID and points of a multidimensional experiment
- 135 6) phase program definitions

#### 136 3.2.1 General modules

137 The general modules fit into this sequential structure as follows:

- 138 1a) configuration and compile-time calculations
- 139 1b) **init.incl**
- 140 1c) configuration and compile-time calculations continued
- 141 2) a "zd" or "ze" statement
- 142 3a) real-time calculations
- 143 3b) **start.incl**
- 144 3c) pulse program body (pulses and delays) and real-time calculations
- 145 4) **end.incl**
- 146 5) loop statements for scans of a FID and points of a multidimensional experiment
- 147 6a) **phasecycles.incl**
- 148 6b) phase program definitions

149 The general modules have numerous conditional statements and imports evaluating the option provided in point 1) above  
150 and using the built-in ZGOPTNS variable and interact with the specific modules (this is covered below). The init.incl

151 module provides the library's core functionality by defining macros for functions and variable descriptions. start.incl  
152 executes the relaxation delay (with possible solvent presaturation) and optional operations, such as crushing residual C or N  
153 magnetization (gradient pulse after an excitation pulse) or inverting N magnetization before the relaxation delay in BEST-  
154 TROSY. For non-protein experiments an ASAP (Kupče and Freeman, 2007) period would be added here, but the relevant  
155 code is experimental and provided in a commented-out form due to the method's potential to damage probeheads. The  
156 end.incl module handles acquisition with the option for real-time homodecoupling - here provided with  $^{13}\text{C}$ -GBIRD<sup>t,x</sup>  
157 (Garbow et al., 1982; Haller et al., 2022) and BASHD (Brüschweiler et al., 1988; Krishnamurthy, 1997) types.

### 158 3.2.2 Specific modules

159 In contrast to the general modules, specific modules implement a specific form of proximal or distal block and serve to  
160 localize the relevant code in a single file. The biggest hurdle to writing self-contained modules for TopSpin is the sequential  
161 pulse program structure necessitating the separation of related code segments in the post-preprocessing file. To mitigate this  
162 problem, each module is entirely enclosed in a conditional statement with alternative conditions (an if...elif...else structure)  
163 and including the file once will only insert a selected part of the module into a file. Since the 4 general modules already  
164 perform the sequential separation of code, each of them sets the appropriate conditions (defines a macro) and imports the  
165 distal\_2D.incl and proximal\_2D.incl which themselves import the selected specific modules at each of the 4 positions in the  
166 pulse program. Thus, the initialization phase statements (variable declarations, some calculations, macro definitions) are  
167 included in init.incl, runtime calculations of both types of modules are included through start.incl, together with the main  
168 body (pulses and delay statements) of the distal. Similarly, the main body of the proximal module is included through the  
169 end.incl before the latter's acquisition portion. Phase cycles of both modules are inserted into a pulse program file through  
170 phasecycles.incl with some basic logic, allowing for coordinating the cycles between them if two modules are used.

171 For triple-resonance experiments (in the implementation limited to amide protons, but should be possible to extend to  
172 aliphatic/aromatic groups) the proximal module hx.incl and the distal module hx.incl provide the ability to compartmentalize  
173 the relatively standard blocks for both out-and-back and straight through type experiments and a more detail description in  
174 the context of a HNCO experiment is provided below. Although sub-optimal in some circumstances the library provides  
175 default 2 step phase cycles for each of the modules, leaving the implementation of 8 step and longer cycles for the central  
176 part of the program. A more detailed description of individual modules is provided in library documentation. In the  
177 supplemental we provide a detailed step-by-step description of the proximal HSQC module and the way it is used in the 2D  
178 experiment pulse program.

179

180 A specific module separate from the proximal-distal type can also be based on the same structure and either manually  
181 included in the pulse program after each general module or in a specific module itself - se.incl is module implementing the  
182 sensitivity-enhanced COS-INEPT and TROSY transfers and is imported in both the hsqc\_se.incl and hx.incl modules.

## 183 4 Application examples

### 184 4.1 HNCO

```
proscl relations=<me>

# include <Avance.incl>
# include <Grad.incl>

# define DIMS 3

/*Select options for distal and proximal blocks:*/
# define XH
# define HX
# define DISTAL_N
# define DISTAL_Y_CO
# define DISTAL_A_CA
# define PROXIMAL_NH
# define PROXIMAL_Y_CO
# define PROXIMAL_A_CA

; Variable definitions for the distal (H->N) and proximal (N->H) blocks:
# include <ME/includes/init.incl>

1 ze

; Relaxation and distal block Hz -> NzHz -> COzNz:
# include <ME/includes/start.incl>

; 2COzNz CO evolution (T1):
(CO_excitation(phFree1)):fCO
T1*0.5
(center (CA_CO_inversion(ph0)):fCA (N_inversion(ph0)):fN)
T1*0.5
(CO_refocussing(ph0)):fCO
(CA_CO_inversion(ph0)):fCA ; BSP compensation.
(CO_flipback(ph0)):fCO

GRAD(gpFree1)

; Proximal block COzNz -> NzHz-> H and acquisition:
# include <ME/includes/end.incl>
F1PH(calph(phFree1,+90), caldel(T1, +in1))
exit

# include <ME/includes/phasecycles.incl>

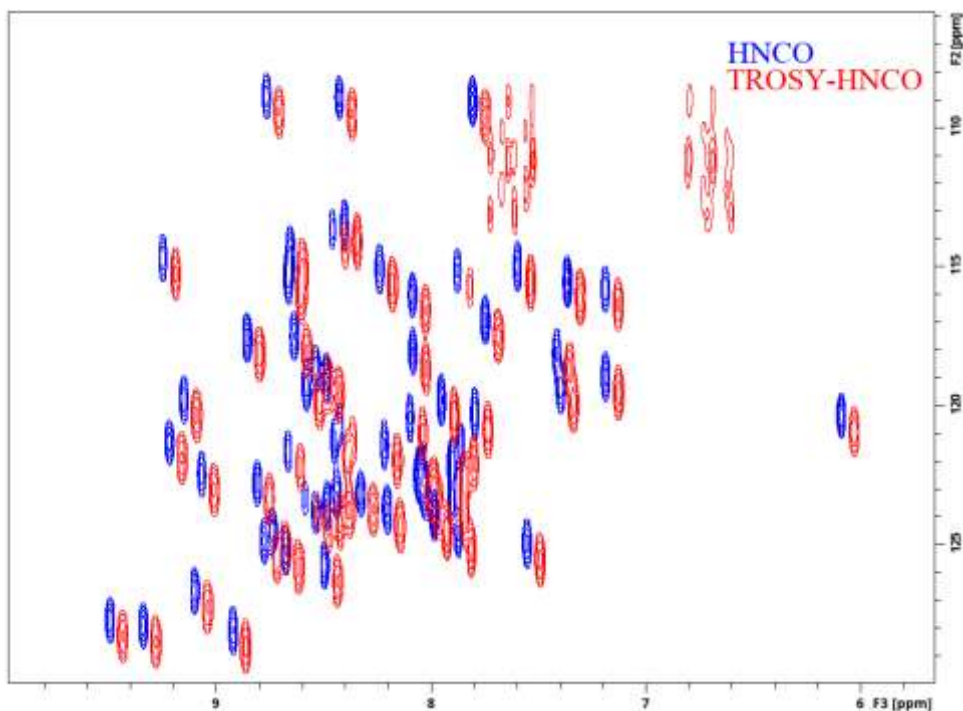
phFree1 = 0 0 0 0 2 2 2 2

; Receiver phase:
phRec = PROXIMAL_PH31 + DISTAL_PH31 + phFree1

;gpzFree1: gradient after CO echo: 21%.

185 ;gpnamFree1: SMSQ10.100
```

186 Fig. 1. Pulse program code for the implementation of the HNCO experiment.

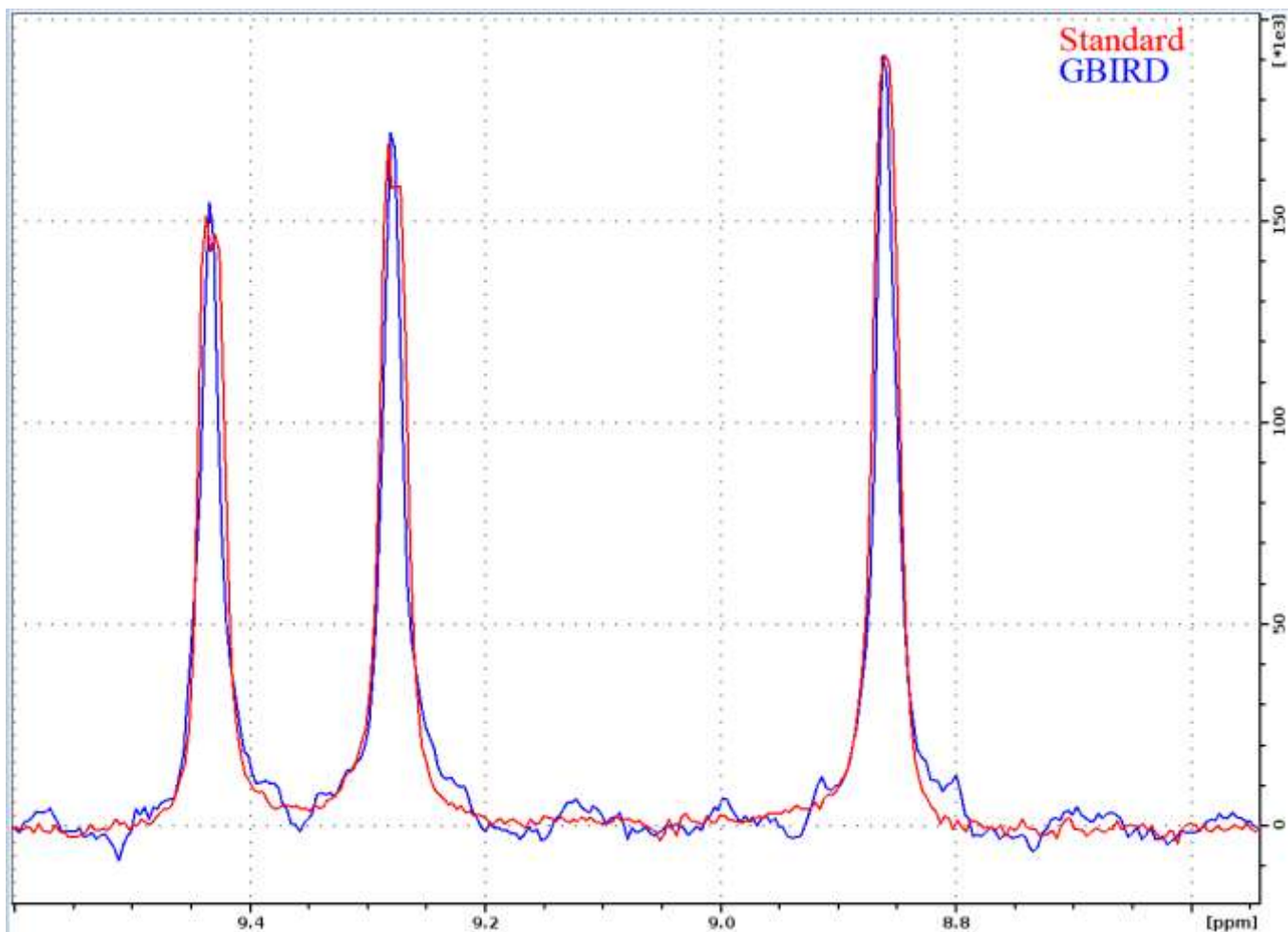


187

188 **Fig. 2. Experimental demonstration of the implementations of the HNCO and TROSY-HNCO experiments for ubiquitin 8 (kDa) at**  
 189 **25 °C. Spectra were recorded as  $^1\text{H}$ - $^{15}\text{N}$  planes with maximum evolution times of 85.2 ms ( $^1\text{H}$ ) and 9.87 ms ( $^{15}\text{N}$ ) and processed**  
 190 **using cosine squared window functions.**

191 HNCO is one of the simplest triple-resonance experiments and thus a good candidate to demonstrate the strengths and  
 192 limitations of the presented approach to library building. We present its ME NMR implementation in Fig. 1. We use a  
 193 custom prosol file (used mostly for automatic precalculation of pulse parameters) to free up a number of variables. Evolution  
 194 delays and increments are defined explicitly due to the proximal module's numbered variables (here *td2* and *in2*) being  
 195 dimensionality-dependant. The block of defines specifies options for ME library - specifying the proximal (*xh.incl*) and  
 196 distal (*hx.incl*) modules and the couplings to be evolved (*Y* is  $^2J_{\text{NCO}}$ ) and decoupled (*A* is  $^2J_{\text{NCA}}$ ). After importing the first two  
 197 general modules, which include the distal modules, two evolution periods, the carbonyl echo is implemented using the  
 198 library's low-level functionality. Since channels and pulses aren't selected explicitly, this block will function with split CA  
 199 and CO channels (with the right spectrometer configurations and "CACO\_SPLIT" defined in ZGOPTNS) or using a single  
 200 carbon channel and frequency-offset pulses. The rest of the pulse program includes the *end.incl* module (with the two  
 201 proximal echoes and acquisition) and standard configuration of gradients and phasecycles. To demonstrate the libraries  
 202 functionality in Fig 2. we present 2D spectra (recorded as HN(CO) experiments) of a standard variant of the experiment (no  
 203 ZGOPTNS) and a TROSY-HNCO (adding the TROSY define to ZGOPTNS) selecting only the  $\text{H}_\beta$  and  $\text{N}_\beta$  component (the  
 204 lower right component using standard display convention). It's possible to choose a  $^{13}\text{C}$ -GBIRD<sup>r,x</sup> appending the  
 205 "ACQ\_BIRD\_C" option to ZGOPTNS, with an example of line narrowing demonstrated in Fig. 3.





206

207 Fig. 3. 1D slices (for  $N = 128.5$  ppm) through  $^1\text{H}$ - $^{15}\text{N}$  planes recorded for a TROSY-HNCO with standard acquisition and  
 208 TROSY-HNCO with  $^{13}\text{C}$ -GBIRD<sup>r,x</sup> demonstrating the effectiveness of the homodecoupling and the resultant line narrowing. Both  
 209 spectra were acquired for ubiquitin 8 (kDa) at 25 °C with maximum evolution times of 340.7 ms ( $^1\text{H}$ ) and 9.87 ms ( $^{15}\text{N}$ ) and  
 210 processed using a cosine squared window function in the N dimension and sine, squared shifted by  $\frac{\pi}{2}$  in the H dimension. The  
 211 GBIRD spectrum was shifted right by 4 Hz (shift was possibly induced by sample heating) and scaled up to match the amplitude of  
 212 the standard TROSY-HNCO. For the GBIRD spectrum, 18 chunks were acquired with a 11.96 ms inter-chunk delay, 3.5 ms  $^2J_{\text{HC}}$   
 213 evolution time and using a 120  $\mu\text{s}$  BIP-720-100-10 (Smith et al., 2001) pulse for  $^{13}\text{C}$  inversion. Linewidths at half height are (from  
 214 left to right) 19.6 Hz, 19.5 Hz and 19.1 Hz for the standard spectrum and 13.2 Hz, 13.2 Hz and 13.7 Hz for the homodecouple  
 215 spectrum (TopSpin peakw function).

216

217

```

prosol relations=<me>

# include <Avance.incl>
# include <Grad.incl>

# define NOESY
# define DIMS 4

; Variable definitions and calculations for the proximal and distal 2Ds:
# include <ME/includes/init.incl>

define delay mixTime
;d10: NOESY mixing time [40-400 ms]
"mixTime = d10 - pGRAD - dGRAD" ; Corrected for gradient.

1 ze

; Distal 2D:
# include <ME/includes/start.incl>

; NOESY mixing:
# ifdef MIX_LOCKED
(
  refalign (mixTime):fH
  lalign (1m 4u BLKGRAD):fH
  ralign (2m UNBLKGRAD):fH
)
# else
  mixTime
# endif

  GRAD(gpNOESY)

; Proximal 2D and acquisition:
# include <ME/includes/end.incl>
exit

# include <ME/includes/phasecycles.incl>

; Receiver phase:
phRec = PROXIMAL_PH31 + DISTAL_PH31

;gpzNOESY: gradient after NOESY: -7%.
;gpnamNOESY: SMSQ10.100

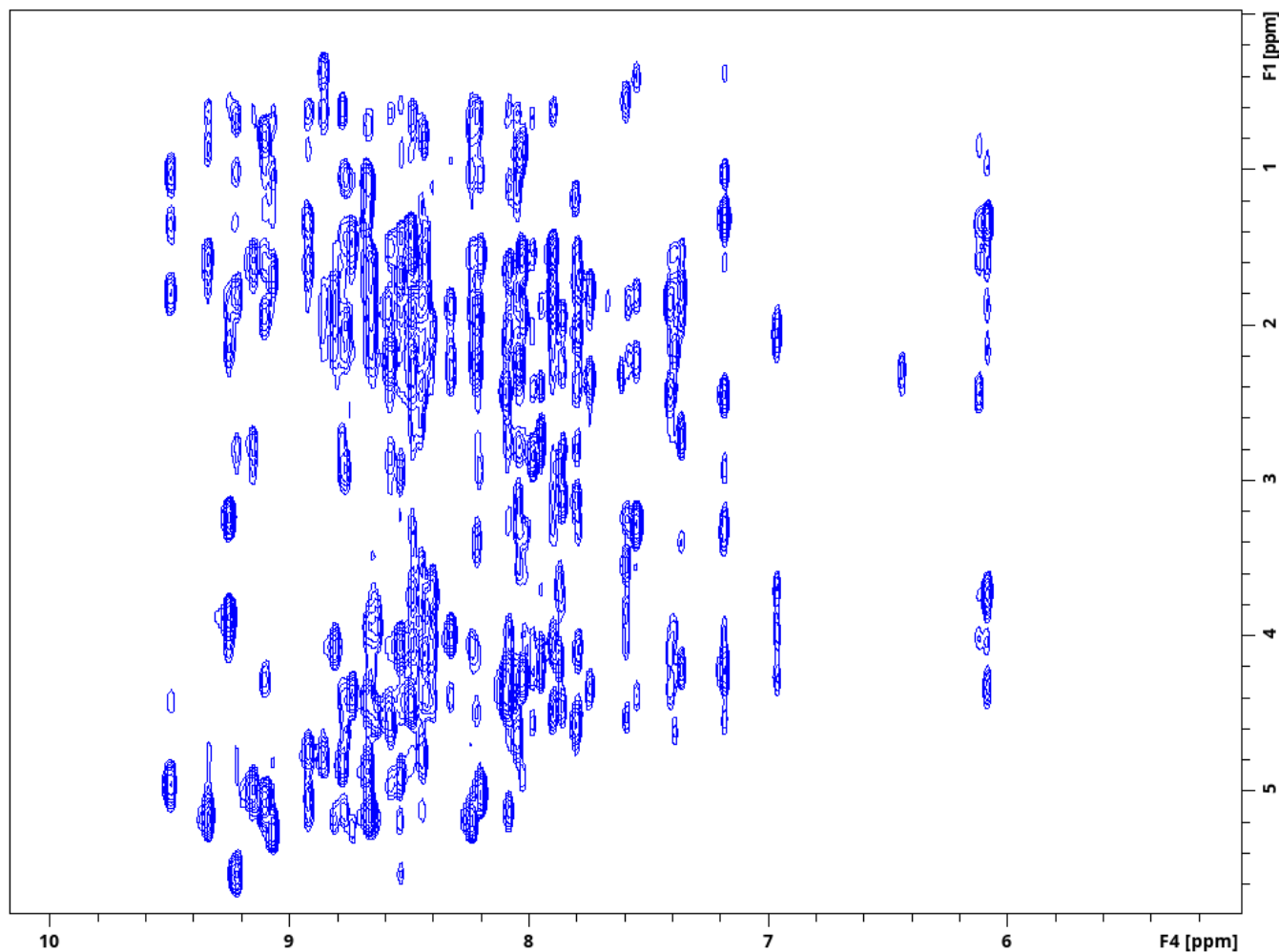
```

219

220 Fig. 4. Pulse program code for the implementation of a 4D NOESY experiment.

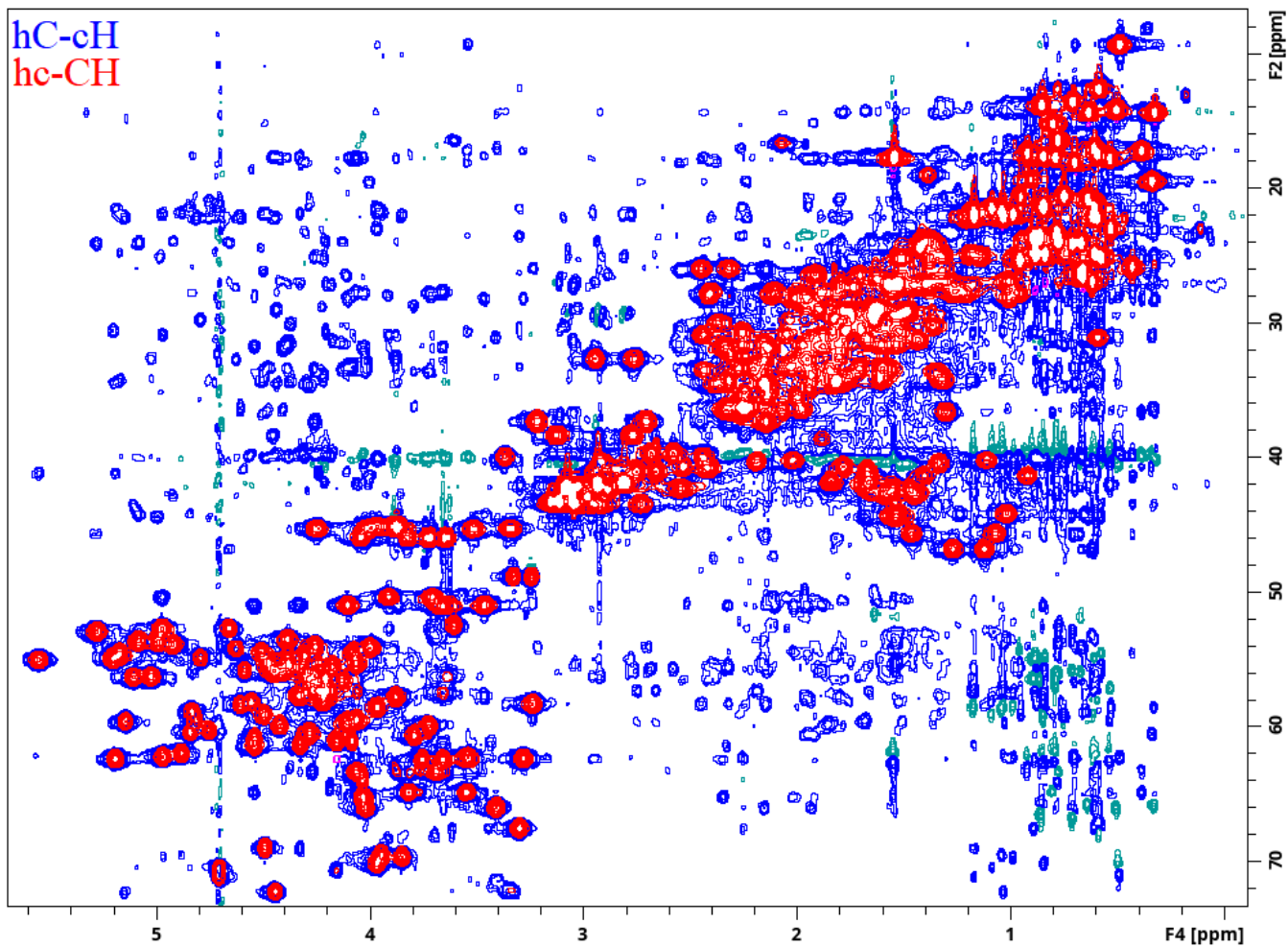
221 The modular nature of the library is exemplified by the 4D NOESY pulse program in Fig. 4. Apart from the basic structure  
222 described above in the case of HNCO it only contains a mixing period joining the proximal and distal module, with the  
223 evolved heteronuclei and experiment types selected by the user using ZGOPTNS. A HC,NH-HMQC-NOESY-HSQC with  
224 sensitivity enhancement in the last dimension (Fig. 5.) can be changed to a HC,CH-HMQC-NOESY-HSQC (Fig. 6.) pulse  
225 program by changing the “PROXIMAL\_N” option to “PROXIMAL\_C” and adding the gradient selection option (“GS”,  
226 which isn’t a default for non-sensitivity-enhanced HSQC.

227

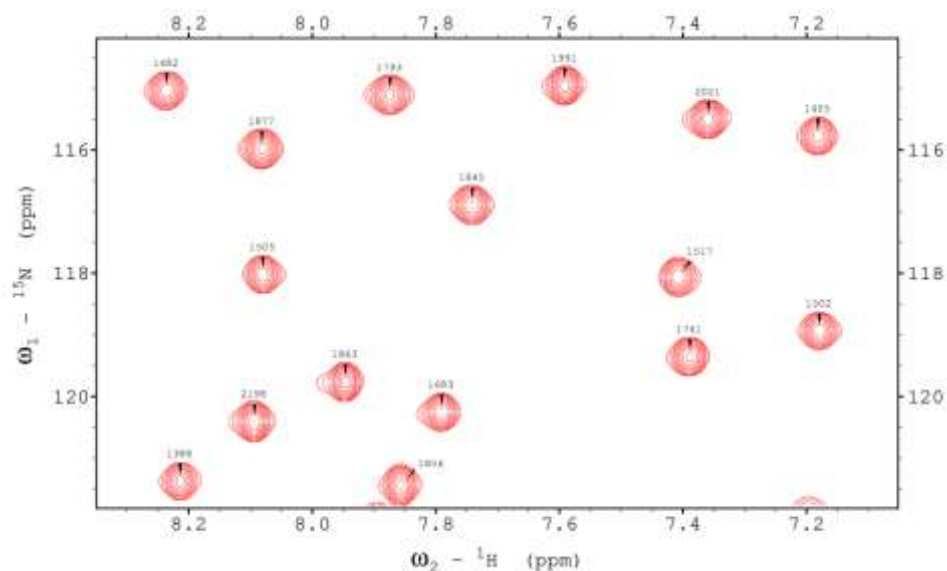


228  
229  
230  
231

**Fig. 5.**  $^1\text{H}$ - $^1\text{H}$  planes recorded using a 4D HC,NH-HMQC-NOESY-HSQC experiment for ubiquitin 8 (kDa) at 25 °C. Spectra were recorded with maximum evolution times of 85,2 ms ( $^1\text{H}$  direct dimension) and 6.99 ms ( $^1\text{H}$  indirect dimension) and processed using cosine squared window functions.

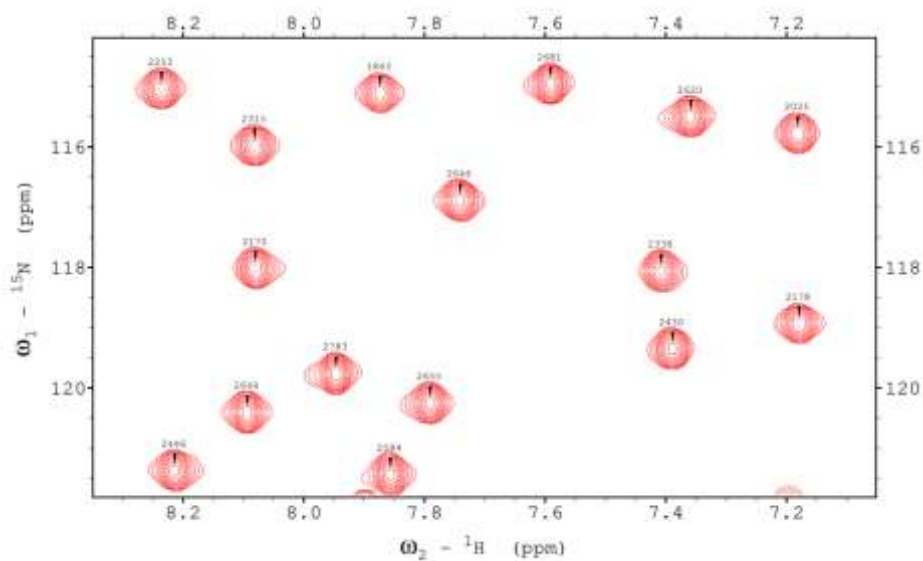


232  
 233 Fig. 6. Two different  $^1\text{H}$ - $^{13}\text{C}$  2D planes recorded using a ME implementation of a 4D HC,CH-HMQC-NOESY-HSQC experiment  
 234 for ubiquitin 8 (kDa) at 25 °C. Spectra were recorded with maximum evolution times of 85.2 ms ( $^1\text{H}$  direct dimension) and 7.96 ms  
 235 (both  $^{13}\text{C}$  dimensions) and processed using cosine squared window functions.



237

238 Fig. 7.  $^1\text{H}$ ,  $^{15}\text{N}$  TROSY spectrum recorded using a ME implementation with hard pulses and water flipback for ubiquitin 8 (kDa) at  
 239 25 °C. The spectrum was recorded with maximum evolution times of 85,2 ms ( $^1\text{H}$ ) and 39,5 ms ( $^{15}\text{N}$ ) and processed using cosine  
 240 squared window functions.



241

242 Fig. 8.  $^1\text{H}$ ,  $^{15}\text{N}$  TROSY spectrum recorded using a ME implementation with shaped pulses (E400B and RE-BURP) for ubiquitin 8  
 243 (kDa) at 25 °C. The spectrum was recorded with maximum evolution times of 85,2 ms ( $^1\text{H}$ ) and 39,5 ms ( $^{15}\text{N}$ ) and processed using  
 244 cosine squared window functions.

245

246 Since BEST-type experiments utilizing shaped pulses can bring improved sensitivity especially at higher scan repetition  
247 rates (Schanda et al., 2006) we demonstrate the library's inherent ability to automatically adapt to the substantial chemical  
248 shift and coupling evolution during the 90-degree universal rotation E400B (Veshtort and Griffin, 2004) (using a time-  
249 reversed version of the original pulse for excitation) pulses with the length of 1073.1  $\mu$ s (equivalent to an ideal pulse  
250 followed by a 611.7  $\mu$ s delay) and refocussing pulse RE-BURP (Geen and Freeman, 1991) with length of 1108.8  $\mu$ s  
251 (modelled as an ideal refocussing pulse flanked by 554  $\mu$ s delays) in Fig. 7. and 8. With a relaxation delay of 0.65 s all peaks  
252 in the selected region are over 20% stronger in the shaped pulse version. Full datasets for a number of different relaxation  
253 delays are provided, as in the data availability section.

## 254 **5 Materials & methods**

255 For all experiments we used a 2 mM  $^{13}\text{C}$ ,  $^{15}\text{N}$ -double labelled human ubiquitin (ASLA Biotech) in a 5 mm Shigemi NMR  
256 microtube. All spectra were acquired using a Bruker Avance IIIHD 800 MHz spectrometer with a 5 mm TCI z-gradient  
257 cryo-probe. Pulse lengths for 90 degree hard pulses were 10.47  $\mu$ s for  $^1\text{H}$ , 12.3  $\mu$ s for  $^{13}\text{C}$  and 33.22  $\mu$ s for  $^{15}\text{N}$ . Full  
258 acquisition and processing parameters are provided in the dataset linked below in the Data availability section. Acquisition  
259 and library testing was, performed using the TopSpin 3.6.5 Service Pack 2 software (Bruker). Data processing and plotting  
260 (aside from Fig. 7. and 8.) was carried out in TopSpin. Figures 7 and 8 were prepared using the NMRFAM-SPARKY  
261 software (Goddard and Kneller, 2004; Lee et al., 2015).

## 262 **6 Conclusions**

263 We have described a framework library implementing a two-level approach to pulse program modularization and  
264 demonstrated its utility. We hope it can be used by others either directly for the streamlining of pulse program code or as an  
265 inspiration for similar frameworks. Although the usefulness of the modularization approach is most obvious for the case of  
266 protein experiments presented here, it should extend to nucleic acids and, to a more limited extent, small molecules. In the  
267 latter case, the ability to modularize preparation period operations (presaturation, ASAP), WATERGATE (Piotto et al.,  
268 1992; Sklenar et al., 1993) type solvent suppression and real-time acquisition should be particularly useful.

## 269 **Code availability**

270 The initial version of the ME library code and documentation is available online at:  
271 <https://doi.org/10.5281/zenodo.10841749>. Current library version is available online at [https://github.com/nmr-](https://github.com/nmr-cnbch/MEnmr_pubcode)  
272 [cnbch/MEnmr\\_pubcode](https://github.com/nmr-cnbch/MEnmr_pubcode) or from the authors upon request.

273 **Data availability**

274 All data used in the preparation of this article is available online at: <https://doi.org/10.5281/zenodo.10578330>.

275 **Author contributions**

276 MG and WK designed the general workflow of the ME library. MG wrote the library code and performed the experiments.

277 MG wrote the manuscript with input from WK.

278

279 **Financial support**

280 This research was supported by the Polish National Science Centre grant PRELUDIUM 2015/19/N/ST4/00863 to MG.

281 **Competing interests**

282 The authors declare that they have no conflict of interest.

283 **References**

284 Asami, S., Kallies, W., Günther, J. C., Stavropoulou, M., Glaser, S. J., and Sattler, M.: Ultrashort Broadband Cooperative  
285 Pulses for Multidimensional Biomolecular NMR Experiments, *Angewandte Chemie*, 130, 14706–14710,  
286 <https://doi.org/10.1002/ange.201800220>, 2018.

287 Bodenhausen, G. and Ruben, D. J.: Natural abundance nitrogen-15 NMR by enhanced heteronuclear spectroscopy, *Chemical  
288 Physics Letters*, 69, 185–189, [https://doi.org/10.1016/0009-2614\(80\)80041-8](https://doi.org/10.1016/0009-2614(80)80041-8), 1980.

289 Brüschweiler, R., Griesinger, C., Sørensen, O. W., and Ernst, R. R.: Combined use of hard and soft pulses for  $\omega_1$  decoupling  
290 in two-dimensional NMR spectroscopy, *Journal of Magnetic Resonance (1969)*, 78, 178–185, [https://doi.org/10.1016/0022-  
291 2364\(88\)90171-0](https://doi.org/10.1016/0022-<br/>291 2364(88)90171-0), 1988.

292 Favier, A. and Brutscher, B.: NMRLib: user-friendly pulse sequence tools for Bruker NMR spectrometers, *J Biomol NMR*,  
293 73, 199–211, <https://doi.org/10.1007/s10858-019-00249-1>, 2019.

294 Garbow, J. R., Weitekamp, D. P., and Pines, A.: Bilinear rotation decoupling of homonuclear scalar interactions, *Chemical  
295 Physics Letters*, 93, 504–509, [https://doi.org/10.1016/0009-2614\(82\)83229-6](https://doi.org/10.1016/0009-2614(82)83229-6), 1982.

296 Geen, H. and Freeman, R.: Band-selective radiofrequency pulses, *Journal of Magnetic Resonance (1969)*, 93, 93–141,  
297 [https://doi.org/10.1016/0022-2364\(91\)90034-Q](https://doi.org/10.1016/0022-2364(91)90034-Q), 1991.

298 Gershenson, N. I., Skinner, T. E., Brutscher, B., Khaneja, N., Nimbalkar, M., Luy, B., and Glaser, S. J.: Linear phase slope  
299 in pulse design: Application to coherence transfer, *Journal of Magnetic Resonance*, 192, 235–243,  
300 <https://doi.org/10.1016/j.jmr.2008.02.021>, 2008.

301 Goddard, T. D. and Kneller, D. G.: SPARKY 3, 2004.

- 302 Haller, J. D., Bodor, A., and Luy, B.: Pure shift amide detection in conventional and TROSY-type experiments of  $^{13}\text{C}$ ,  $^{15}\text{N}$ -  
303 labeled proteins, *J Biomol NMR*, 76, 213–221, <https://doi.org/10.1007/s10858-022-00406-z>, 2022.
- 304 Ikura, M., Kay, L. E., and Bax, A.: A novel approach for sequential assignment of  $^1\text{H}$ ,  $^{13}\text{C}$ , and  $^{15}\text{N}$  spectra of proteins:  
305 heteronuclear triple-resonance three-dimensional NMR spectroscopy. Application to calmodulin, *Biochemistry*, 29, 4659–  
306 4667, 1990.
- 307 Kay, L. E., Clore, G. M., Bax, A., and Gronenborn, A. M.: Four-dimensional heteronuclear triple-resonance NMR  
308 spectroscopy of interleukin-1 beta in solution, *Science*, 249, 411–414, <https://doi.org/10.1126/science.2377896>, 1990a.
- 309 Kay, L. E., Ikura, M., Tschudin, R., and Bax, A.: Three-dimensional triple-resonance NMR spectroscopy of isotopically  
310 enriched proteins, *Journal of Magnetic Resonance (1969)*, 89, 496–514, [https://doi.org/10.1016/0022-2364\(90\)90333-5](https://doi.org/10.1016/0022-2364(90)90333-5),  
311 1990b.
- 312 Kazimierczuk, K., Zawadzka-Kazimierczuk, A., and Koźmiński, W.: Non-uniform frequency domain for optimal  
313 exploitation of non-uniform sampling, *Journal of Magnetic Resonance*, 205, 286–292,  
314 <https://doi.org/10.1016/j.jmr.2010.05.012>, 2010.
- 315 Krishnamurthy, V. V.: Application of Semi-Selective Excitation Sculpting for Homonuclear Decoupling During Evolution in  
316 Multi-Dimensional NMR, *Magnetic Resonance in Chemistry*, 35, 9–12, [https://doi.org/10.1002/\(SICI\)1097-  
317 458X\(199701\)35:1<9::AID-OMR930>3.0.CO;2-R](https://doi.org/10.1002/(SICI)1097-458X(199701)35:1<9::AID-OMR930>3.0.CO;2-R), 1997.
- 318 Kupče, E. and Freeman, R.: Fast multidimensional NMR by polarization sharing, *Magnetic Resonance in Chemistry*, 45, 2–  
319 4, <https://doi.org/10.1002/mrc.1931>, 2007.
- 320 Lee, W., Tonelli, M., and Markley, J. L.: NMRFAM-SPARKY: enhanced software for biomolecular NMR spectroscopy,  
321 *Bioinformatics*, 31, 1325–1327, <https://doi.org/10.1093/bioinformatics/btu830>, 2015.
- 322 Lescop, E., Kern, T., and Brutscher, B.: Guidelines for the use of band-selective radiofrequency pulses in hetero-nuclear  
323 NMR: Example of longitudinal-relaxation-enhanced BEST-type  $^1\text{H}$ – $^{15}\text{N}$  correlation experiments, *Journal of Magnetic  
324 Resonance*, 203, 190–198, <https://doi.org/10.1016/j.jmr.2009.12.001>, 2010.
- 325 Lukavsky, P. J. and Puglisi, J. D.: RNAPack: An Integrated NMR Approach to RNA Structure Determination, *Methods*, 25,  
326 316–332, <https://doi.org/10.1006/meth.2001.1244>, 2001.
- 327 Nietlispach, D.: Suppression of anti-TROSY lines in a sensitivity enhanced gradient selection TROSY scheme, *J Biomol  
328 NMR*, 31, 161–166, <https://doi.org/10.1007/s10858-004-8195-7>, 2005.
- 329 Palmer, A. G., Cavanagh, J., Wright, P. E., and Rance, M.: Sensitivity improvement in proton-detected two-dimensional  
330 heteronuclear correlation NMR spectroscopy, *Journal of Magnetic Resonance (1969)*, 93, 151–170,  
331 [https://doi.org/10.1016/0022-2364\(91\)90036-S](https://doi.org/10.1016/0022-2364(91)90036-S), 1991.
- 332 Piotto, M., Saudek, V., and Sklenář, V.: Gradient-tailored excitation for single-quantum NMR spectroscopy of aqueous  
333 solutions, *J Biomol NMR*, 2, 661–665, <https://doi.org/10.1007/BF02192855>, 1992.
- 334 Salzmann, M., Wider, G., Pervushin, K., and Wüthrich, K.: Improved sensitivity and coherence selection for  $[^{15}\text{N}, ^1\text{H}]$ -  
335 TROSY elements in triple resonance experiments, *J Biomol NMR*, 15, 181–184, <https://doi.org/10.1023/A:1008358030477>,  
336 1999a.



- 337 Salzman, M., Wider, G., Pervushin, K., Senn, H., and Wüthrich, K.: TROSY-type Triple-Resonance Experiments for  
338 Sequential NMR Assignments of Large Proteins, *J. Am. Chem. Soc.*, 121, 844–848, <https://doi.org/10.1021/ja9834226>,  
339 1999b.
- 340 Schanda, P., Van Melckebeke, H., and Brutscher, B.: Speeding Up Three-Dimensional Protein NMR Experiments to a Few  
341 Minutes, *J. Am. Chem. Soc.*, 128, 9042–9043, <https://doi.org/10.1021/ja062025p>, 2006.
- 342 Schulte-Herbrüggen, T. and Sørensen, O. W.: Clean TROSY: Compensation for Relaxation-Induced Artifacts, *Journal of*  
343 *Magnetic Resonance*, 144, 123–128, <https://doi.org/10.1006/jmre.2000.2020>, 2000.
- 344 Sklenar, V.: Suppression of Radiation Damping in Multidimensional NMR Experiments Using Magnetic Field Gradients,  
345 *Journal of Magnetic Resonance, Series A*, 114, 132–135, <https://doi.org/10.1006/jmra.1995.1119>, 1995.
- 346 Sklenar, V., Piotto, M., Leppik, R., and Saudek, V.: Gradient-Tailored Water Suppression for <sup>1</sup>H-<sup>15</sup>N HSQC Experiments  
347 Optimized to Retain Full Sensitivity, *Journal of Magnetic Resonance, Series A*, 102, 241–245,  
348 <https://doi.org/10.1006/jmra.1993.1098>, 1993.
- 349 Smith, M. A., Hu, H., and Shaka, A. J.: Improved Broadband Inversion Performance for NMR in Liquids, *Journal of*  
350 *Magnetic Resonance*, 151, 269–283, <https://doi.org/10.1006/jmre.2001.2364>, 2001.
- 351 Solyom, Z., Schwarten, M., Geist, L., Konrat, R., Willbold, D., and Brutscher, B.: BEST-TROSY experiments for time-  
352 efficient sequential resonance assignment of large disordered proteins, *J Biomol NMR*, 55, 311–321,  
353 <https://doi.org/10.1007/s10858-013-9715-0>, 2013.
- 354 Sprangers, R. and Kay, L. E.: Quantitative dynamics and binding studies of the 20S proteasome by NMR, *Nature*, 445, 618–  
355 622, <https://doi.org/10.1038/nature05512>, 2007.
- 356 Stallman, R., M. and GCC Developer Community: Using the GNU Compiler Collection, Free Software Foundation, Boston,  
357 2012.
- 358 Vallet, A., Favier, A., Brutscher, B., and Schanda, P.: ssNMRLib: a comprehensive library and tool box for acquisition of  
359 solid-state nuclear magnetic resonance experiments on Bruker spectrometers, *Magnetic Resonance*, 1, 331–345,  
360 <https://doi.org/10.5194/mr-1-331-2020>, 2020.
- 361 Veshtort, M. and Griffin, R. G.: High-Performance Selective Excitation Pulses for Solid- and Liquid-State NMR  
362 Spectroscopy, *ChemPhysChem*, 5, 834–850, <https://doi.org/10.1002/cphc.200400018>, 2004.
- 363 Yang, D. and Kay, L. E.: TROSY Triple-Resonance Four-Dimensional NMR Spectroscopy of a 46 ns Tumbling Protein, *J.*  
364 *Am. Chem. Soc.*, 121, 2571–2575, <https://doi.org/10.1021/ja984056t>, 1999.
- 365 Yong, J. R. J., Kupče, E., and Claridge, T. D. W.: Modular Pulse Program Generation for NMR Supersequences, *Anal.*  
366 *Chem.*, 94, 2271–2278, <https://doi.org/10.1021/acs.analchem.1c04964>, 2022.
- 367 Zawadzka-Kazimierczuk, A.: New methods of protein NMR spectra analysis using the techniques of high dimensionality,  
368 Doctoral dissertation, University of Warsaw, 2012.
- 369